Microstructure by Thermal Analysis

D.A. Sparkman
MeltLab Systems, Winchester, VA

ABSTRACT

Thermal analysis has come a long way since its inception. With modern high speed computers, higher precision thermal couple readings, and good mathematical procedures, it is now possible, by using higher order derivatives, to measure the energy signatures of different phases and structures in iron and aluminum and interpret them into usable chemistry and microstructure readings. The advantage is to have high quality information on the foundry floor within minutes of sampling while reducing the turnaround time of the laboratory to just a few minutes.

In this paper the 2nd, 3rd, 4th, and 5th derivatives will be used to delimitate multiple arrests in aluminum and iron, so that the energy of those phases can be measured, and a new test will be introduced for nodularity based on the smoothness of the energy production of the different forms of graphite. Finally, the problem of shrinkage in ductile iron will be revisited in the form of the balance of energy from the thermal analysis curve. All of these new tools are derived from the use of higher derivatives and the integration of the energy flows found through thermal analysis.

The calculation of higher order derivatives presents a problem of signal filtering to remove the noise without losing the data. This has finally been accomplished in a computer system. What remains is to understand and interpret what can now finally be clearly seen.

Key Words: thermal analysis, higher order derivatives, energy integration, microstructure, ductile iron, stress energy, shrinkage, aluminum

INTRODUCTION

A thermal analysis curve is a measurement of the crystallization of a sample of metal that can be compared with a casting. It has a mass, a section size, a cooling rate, and a chemistry sampled from the metal at a stage in the casting operation. If that point of sampling reflects the metal entering the casting cavity with all the inoculation and modifications typical of that casting, then, within the limits of the cooling rates and section sizes, a comparison of the microstructure of the casting can be reasonably expected to be seen in the microstructure of the thermal analysis sample.

Where cooling rates promote different microstructures such as in thin sections, it has still been common to use a standardized slug of metal cast in a separate mold or in the actual casting mold itself to serve as a representative sample to check for proper metal preparation. Only in the extreme case in certain life and limb castings is an actual casting destroyed to prove proper microstructure.

Ultrasonic testing of castings has been used to check for nodularity control in ductile iron for many years, and is an accepted practice in many foundries. Recently, the Ductile Iron Society has undertaken research in the use of a nodularity coupon and ultrasonics as a way to automate the testing and remove some of the human interpretation of the results [Ref 27]. Likewise, several thermal analysis characteristics have been looked at over the years as a way of qualifying microstructure. The AluDelta (trademark of Siedermes) instrument started measuring grain fineness values in inoculated aluminum [Ref 29], and considerable work has been done by Bäckerud on the understanding of aluminum nucleation and modification [Ref 30]. NovaCast spent considerable time researching the tendencies of ductile iron to shrink, and built an instrument, the ATAS (trademark of NovaCast), around that research.

While several researchers are looking to extend the benefits of thermal analysis [Ref 1, 2, 3, 12, 13, 15, 18, 20, 25, 28, 29, 30], there is only so much information that can be extracted by measuring the common arrest points. This paper is a discussion of the next logical step in utilizing thermal analysis as a production tool, and that is to introduce higher order derivatives to enable the measurement of the energy signatures of different microstructures. With this information, it should become possible to calculate the amounts of different phases in the sample casting. Admittedly, this is not a substitute for a complete microstructure, where a casting is dissected in its various section thicknesses. But it can be a quick and efficient check on a process, and possibly tell if there has been an adverse change in the process that needs correction.

CONCEPT

Most metals are composed of various phases that precipitate out at different temperatures. Each phase produces a heat signature [Ref 25] that alters the shape of the thermal analysis curve. The inflection may be miniscule but, with

precision equipment, it can be measured and quantified. To do this, a form of mathematics called Calculus is used. The study of Calculus generally is divided into two parts, the study of the rate of change: Derivative Calculus; and the study areas: Integral Calculus. The first type can be used to find and define the beginning and ending of a phase arrest, and the second type can be used to measure the heat energy of the phase, which with a little mathematical magic can be turned into the percent of that phase that will be found under a microscope.

APPLICATION

The first step is to take a phase arrest, and determine the start and end points. Figure 1 is an example of such an arrest in a simple environment: beta crystals in an aluminum-silicon alloy containing 0.4% Fe. The arrest is totally invisible in the temperature part of the curve, but can be seen clearly in the cooling rate (1/1st derivative) curve.

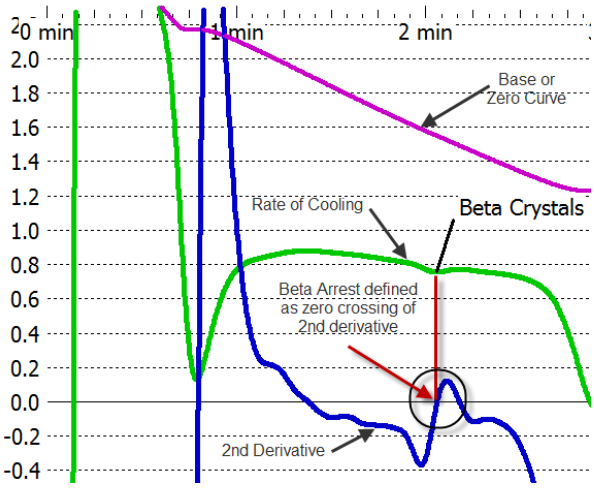

Fig. 1. Beta Arrest inflection point in an aluminum alloy defined by 2nd derivative crossing zero. Rate-of-cooling curve in green, 2nd derivative in blue, zero-curve in magenta.

The bending of the green rate-of-cooling curve first in a clockwise direction, and then in a counter-clockwise direction causes the 2nd derivative to change direction and pass through zero at the moment that the green curve changes to a counter-clockwise direction. This zero crossing point thus defines the strongest point of the beta phase arrest and usually defines the temperature of the arrest.

But with higher order derivatives, it becomes possible to learn a lot more about the beta phase in this sample of metal [Ref 7].

In Fig. 2, the arrest is enlarged and the 5th derivative is shown in cyan (light blue). For some 35 seconds before the arrest event, the 5th derivative is being very quiet. Then something happens and the derivative makes a sharp turn upward through zero, goes down and back up again, and finally returns to zero and settles down again. If the beginning and ending of the strong fluctuation are used as start and stop points for the energy area, the area can be defined by taking the value of the rate of cooling curve at the start and stop points, drawing a straight line between the points and integrating (measuring) the area between that straight line and the rate of cooling curve!

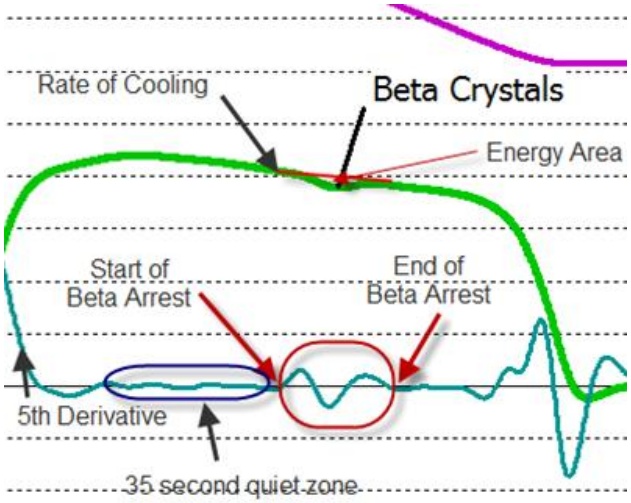

Fig. 2. The higher order 5th derivative, shown here in cyan, defines the area of the arrest, and provides a statistical proof of the arrest.

For accuracy, this calculation is done taking each individual temperature measurement, calculating each rate of cooling measurement and doing the integration with pure numbers. Measuring the visual area on the screen in pixels would lead to too much loss through rounding. It has been asked: why use the fifth derivative? In truth, each derivative beyond the second derivative moves its individual zero crossings closer to what the human eye would pick out as the inflection point. So, the 4th is better than the 3rd, and the 5th is better than the 4th. It was felt that the difference between the 5th and the 6th derivatives was becoming inconsequential and the process could be truncated safely at the 5th. In some difficult phase arrests, truncation is required at the 4th because other arrests are beginning to overlap the arrest being measured [Ref 5].

Another characteristic of the thermal analysis curve shows itself in the 35 second quiet zone shown in Fig. 2. Some will question the ability to measure such a small arrest, so a statistical test would be helpful. There are areas of the curve where nothing is happening, and this is one of them. The time of 35 seconds is not significant, but shows that this period is persistent and can be relied upon as a good measure of the overall background noise. For practical purposes, the 100 data points before the beginning of the arrest are used to calculate a standard deviation of the background signal. This represents 11 seconds of time at the system's 9 readings per second. This can then be compared to the strongest deviation of the 5th derivative during the arrest. In this case the resulting ratio of standard deviation (one sigma) to signal was 5.1: a clearly

real event. Over a period of a month, this experiment produced readings whose statistical certainties ranged from 3.9 sigma to 15.8 sigma [Ref 7].

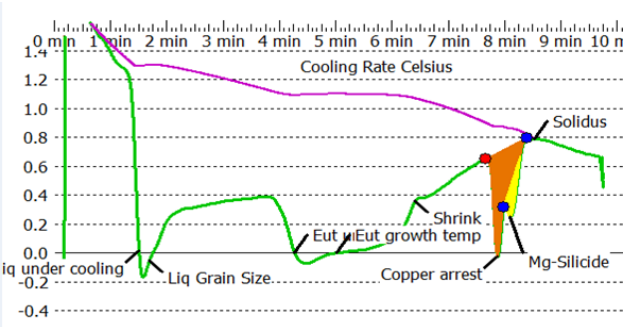

Fig. 3. The total energy of solidification is the area between the magenta zero curve and the green rate of cooling curve. The copper arrest and the magnesium silicide arrest areas are highlighted in copper and yellow colors.

The last piece of data required is the overall energy of solidification. The zero-curve or base line curve helps define the total energy. By integrating the total area between the zero-curve and the rate of cooling curve, we can produce an area representing the total degree-seconds of energy. Some consideration might be taken of the heat extracted, and hence not measured, due to the shrinkage arrest. The results of this measuring technique were applied to a bath of aluminum over a period of a month with the energy area ranging as low as 0.031% at 3.9 standard deviations from background noise. That would suggest that the limits of measurement at the 95% confidence level (2 sigma) would be on the order of 0.01% for that installation: a standard that would be difficult to meet with a microscope.

LATENT HEAT

The final problem in this sample was factoring in the latent heat of beta crystals. Each different phase can be assumed to have a different latent heat or energy. This is the amount of energy released by the solidification of a gram of the material at the temperature at which it solidifies.

While these numbers are understood, very little hard data is available on specific phases [Ref 1]. Typically the latent heat of a given alloy, such as A356 or ferritic ductile iron, is known, but the specific heat of individual phases is not.

A solution would be to introduce a correction for the variation of the phase's latent heat from the overall alloy. In the case of this aluminum, a correction factor of 2.5 times the percent energy of this beta phase gives a very good estimate of the total iron content. Of course, some iron was adsorbed in other phases, but the technique provides a good estimate of total iron when the manganese and magnesium contents are consistent. And if those two elements overwhelm the iron content, as they should in most alloys, there is no beta phase arrest to be measured. A similar technique could also be used to generate a correction factor to calculate the surface area of the beta phase on a microscopic examination or the volume of the phase.

COMPLEX PHASE BOUNDARIES IN ALUMINUM ALLOYS

Similar techniques have been used to look at the microstructures of the copper and magnesium silicide arrests in A356 alloys as shown in Fig. 3 [Ref 6]. In this case, the arrests overlap, and a judgment was made to divide the area of the arrest at the obvious point, but the overall combined arrests can still be defined by the 5th derivative, and the 3rd derivative not only defines the strongest point of each phase, but also defines the separation point between the two phases. In Fig. 4, the positive zero pass of the 5th derivative defines the start of the combined arrest, and the return to zero defines the end of the combined arrest. The positive-going zero crossing of the 3rd derivative in Fig. 5 defines the separation point of the two phases. From there it is only a matter of calculating an approximation of the separation between the eutectic phase and the combined arrest, and a calculating a separation line between the two phases. The rest is integral math as before, and the result is a percent of the total energy of solidification. Add in a correction factor to adjust for specific heat, and the result is an estimate of the percent of each phase present in the sample.

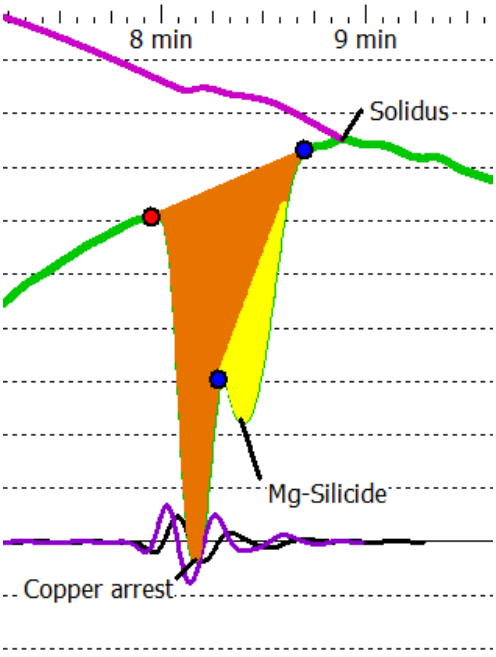

Fig. 4. The zero crossings of the 5th derivative, shown in purple, defines the beginning and ending of the combined arrest, while the 3rd derivative, shown in black, defines the strongest points of each phase as well as the separation point between the phases.

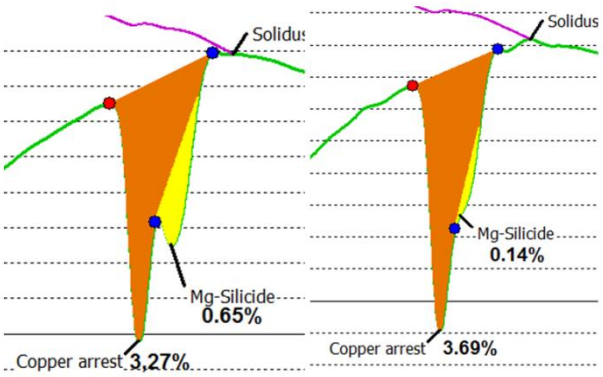

Fig. 5. Here are two separate aluminum curves showing the integrated area of copper and magnesium silicide phases and the percent energy of each. The values seem very close to the actual phase content.

NEGATIVE ENERGY ARRESTS

As is shown in figures 3 and 6, shrinkage can also be seen as the inverse of a phase arrest. Shrinkage can be thought of as the formation of an internal surface. This requires the separation of atoms to form this surface and is endothermic in nature. It removes heat from the system rather than the usual phase crystallization that adds heat energy. The arrest appears similar to other phase arrests except that the direction of the derivatives is flipped.

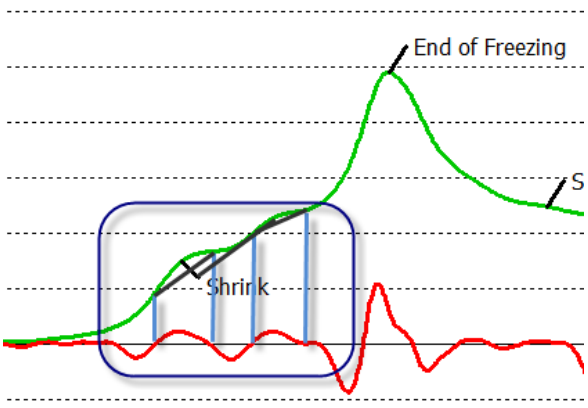

Fig. 6. Here a double shrink has occurred. The upward movement of the cooling rate in green indicates endothermic arrests. The 5th derivate in red can be used to mark the start and end of each arrest allowing the negative energy to be measured.

Shrinkage arrests occur when the casting wall strength is sufficient to resist the stresses set up by the volume loss of the casting. When walls are weak, a suck-in occurs where the casting wall is literally sucked into the casting and the shrinkage volume become external. Suck-ins do not show up as arrests.

Eutectic noise in final ductile and grey irons

For some time, researchers have struggled to find a correlation among some thermal arrest or relationships of arrests and the nodularity of iron. Recently, there has been some interesting research suggesting that vermicular is formed from degraded nodules. It is suggested that spheroidal graphite grows either between dendritic arms in an enriched liquid, and then continues to grow in the austenite, or starts in an austenite shell [Ref 26]. What if, instead of trying to use massive correlations, there was a direct way to see the growth of graphite? Higher derivatives again offer a useable measurement by examining the smoothness of the graphite growth during the eutectic arrest.

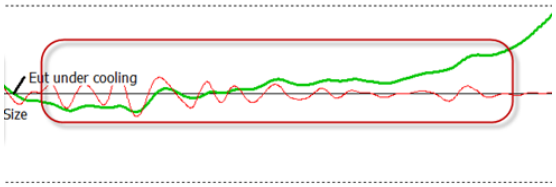

Fig. 6. This is the eutectic portion of an 85% nodularity ductile iron thermal analysis curve with the rate of cooling in green, and the 5th derivative in red. The scale is +/- 1 degree C. The red scale is +/- 0.01 degree C per second4.

Eq. 1 Nodularity = m * ln(StdDev) + b
Where StdDev = Sqrt(Sum(Sqr(5th Derivative))/(n-1))
And n = number of data points

Applying the standard deviation test to the 5th derivatives in figures 6 and 7, an equation of the form of equation 1 seems to fit well from the 99% down to about 75% nodularity. The constants M and B are calculated based on the level of electronic background noise of the individual system, and the local expert's reading of nodularity. Below that, the "StdDev" factor blows up, possibly due to D&E flake and massive carbide growth. It is believed that

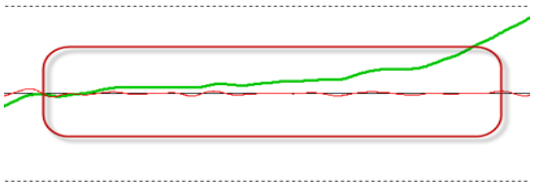

Fig. 7. This is the eutectic portion of a 95% nodularity ductile iron thermal analysis curve with the rate of cooling in green, and the 5th derivative in red. The green scale is +/- 1 degree C. The red scale is +/- 0.01 degree C. Note how much more "quiet" the 5th derivative is.

what is being seen is the steady, consistent growth rate of spheroids, verses the more explosive on-again off-again growth of vermicular graphite.

The same concept appears to hold true in inoculated grey iron as well, with poorly inoculated iron having a larger standard deviation factor than well inoculated iron, though the noise factor is much larger in grey than in ductile.

THE PROBLEM OF STRESS IN DUCTILE IRON

As was seen in the shrinkage arrest, there is an unusual endothermic feature in treated and inoculated ductile iron. At the point of grain boundary solidification or solidus, there is usually an endothermic part of the cooling curve. This does not appear to be a shrinkage arrest, and cutting samples with strong endothermic arrests proves just the opposite: they are generally solid or have just minor micro-shrinkage. On the other hand, samples with little or no endothermic area at the solidus point are those with shrinkage defects or obvious suck-in defects, some (Fig. 9) even to the point of showing a shrinkage arrest on the thermal analysis curve.

This area of stress needs to be explained in terms of physics. Stress or strain energy can be stored in the cell boundaries by decreasing the tightness of the packing of the atoms between grains. Then, as the carbon continues to diffuse to the graphite nodules, an internal hydrostatic pressure is created that causes the atoms in the grain boundaries to repack and reduce that stress. The phase diagram suggests that the carbon content of the eutectic material is about 2.1% at the end of the eutectic solidification. This carbon then drops down to close to zero in a ferritic grade ductile and somewhere near 0.8% in a 100% pearlitic grade. The volume change that the eutectic material undergoes at solidus is not matched by the graphite growth until closer to the eutectoid temperature. Based on the maximum amount of stress energy generated, the volume of austenite, the volume of the precipitated graphite, and the observation that shrinkage can often reach 1% of volume, it would seem that there is indeed a 1% volume difference being made up by the stress at the solidus arrest.

This volume difference will vary of course with different levels of carbon, with less volume difference for higher carbon irons. Depending on the strength of the casting walls, either stress will be set up, or a suck-in will occur. Or, if insufficient volume exists due to poor gating design, choked off gates due to dendrites, early graphite formation feeding the risers (a graphite liquidus), internal gas, or insufficient carbon, then shrinkages or voids will form to relieve the stress before the post-solidus graphite can be formed. If shrinkage occurs, then the post-solidus graphite will enlarge the casting by up to one percent, collapsing a little of the shrinkage, but not seriously fixing the problem.

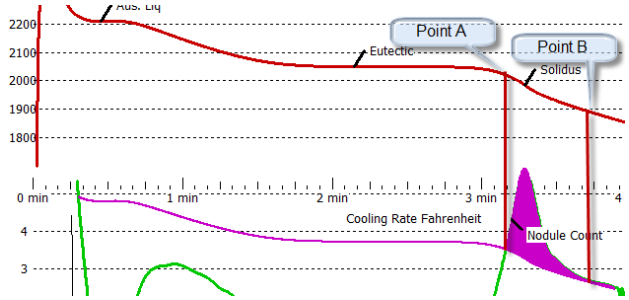

Fig. 8. This sample shows a highly stressed solidus point with a large negative energy area under the solidus, but the sample showed no sign of shrinkage.

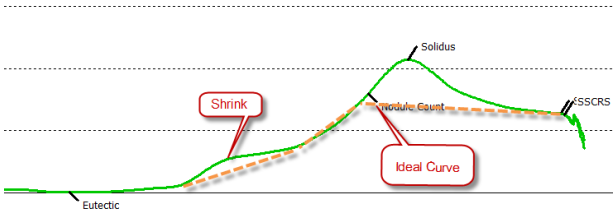

Fig. 9. This sample shows a lesser stressed solidus point with a smaller negative energy area under the solidus, and includes a shrinkage arrest. The total area under the shrink, plus the area under the solidus, is about the same as under the solidus in figure 8.

CONCLUSION

Higher order derivatives offer the possibility of opening up thermal analysis to becoming much more than just a quick chemistry/inoculation check. With the ability to actually measure the energy of individual phases, shrinkage, and stress, many more characteristics of the metal become available for foundry floor measurement. In addition, measuring the "activity" of graphite growth can provide a quick, 3-minute test on nodularity. These advances are made possible by mathematical advances in signal processing, and attention to sampling details.

Many other features of thermal analysis curves remain to be discovered and quantified: iron carbides, gas bubbles, and copper-based alloy phases, to name just a few. The next few years should see an explosion in research using higher level derivatives.

ACKNOWLEDGMENTS

I am indebted to Dick Heine and William Shaw for encouraging me to get into thermal analysis, Carl Loper for showing me the significance of the solidus inflection, for the challenge of Doru Stefanescu, so many years ago to prove that the stress in the solidus was significant, and his

help and the help of W.T. Kierkus and Jerry Sokolowski in mastering the complexities of the zero-curve.

REFERENCES

1. **Mile B. Djurdjevic, Jasey Chen and Jerry H. Sokolowski, "A Novel Algorithm for the Calculation of Latent Heat of Solidification for Multi-Component Aluminum Alloys" American Foundry Society, Des Plaines, IL (2003).**
2. **P. Larrañaga, J. M. Gutiérrez, A. Loizaga, J. Sertucha, R. Suárez, Engineering and Foundry Dept., Azterlan Metallurgical Center, Durango (Bizkaia), Spain "A Computer-Aided System for Melt Quality and Shrinkage Propensity Evaluation Based on the Solidification Process of Ductile Iron" American Foundry Society, Des Plaines, IL (2008).**
3. **M.D. Chaudhari, R.W. Heine, C.R. Loper, Jr. "Principles involved in the use of cooling curve in ductile iron process control" American Foundry Society, Des Plaines, IL (1996)**
4. **D. Sparkman "Hot Topics – Ductile Nodularity", http://www.meltlab.com/hottopics/september2010hottopic.pdf MeltLab Hot Topics (2010)**
5. **D. Sparkman "Quantifying an Arrest in ThermalAnalysis", http://www.meltlab.com/hottopics/august2010quantifiingarrests.pdf MeltLab Hot Topics (2010)**
6. **D. Sparkman "Measuring Microscopic phases using Copper and Magnesium-silicide as an example", http://www.meltlab.com/hottopics/ august2010hottopic.pdf MeltLab Hot Topics (2010)**
7. **D. Sparkman "Measuring Microscopic phases using Aluminum Beta Crystals as an example", http://www.meltlab.com/hottopics/july2010htopic.pdf MeltLab Hot Topics (2010)**
8. **D. Sparkman "Balancing graphite growth and shrinkage in ductile iron", http://www.meltlab.com/hottopics/june2010htopic.pdf MeltLab Hot Topics (2010)**
9. **D. Sparkman "Improving the Accuracy of Thermal Analysis", http://meltlab.com/research/improvingtheaccuracyofthermalanalysis.pdf MeltLab Research Papers (2006)**
10. **D. Sparkman "Offsetting shrinkage in ductile iron – what thermal analysis shows", http://meltlab.com/research/offsettingshrink age-inductileironver2.pdf First published Ductile Iron Society (2001), revised MeltLab Research Papers (2006)**
11. **Chisamera, M; Riposan, I, Stan, S; Sparkman, D; Kelley, D; Barstow, M, "Experience producing compacted graphite cast irons by sulfur addition after magnesium treatment", Journal: Transactions of the American Foundry Society V 110 Paper No 02-007 P 851-859, 2002 (9 p)**
12. **Nafisi, S; Ghomashchi, R; Hedjazi, J; Boutorabi, S M A, "New approaches to melt treatment of Al-Si alloys: application of thermal analysis technique", Journal: Transactions of the American Foundry Society V 112 Paper No 04-018 P 165-177, 2004 (13 p)**
13. **Thomson, J P; Sadayappan, M; Sahoo, M "Evaluation of grain refinement of leaded yellow brass (C85800) and envirobrass III (C89550) using thermal analysis", Journal: Transactions of the American Foundry Society V 111 Paper No 03-119 P 417-434, 2003 (18 p)**
14. **Suarez, O M; Loper, Jr., C R , "Chill wedge test and chilling tendency in gray cast irons", Journal: Transactions of the American Foundry Society V 109 Paper No 01-010 P 1-11, 2001 (11 p)**
15. **Li, H; Griffin, R D, "Evaluating cast iron microstructures using density measurements", Journal: Transactions of the American Foundry Society V 111 Paper No 03-034 P 703-714, 2003 (12 p)**
16. **Chisamera, M., Stan, S., Riposan, I., Costache, G., Barstow, M., "Solidification Pattern of In-Mold and Ladle Inoculated Low Sulfur Hypoeutectic Gray Cast Irons", Journal: AFS Transactions 2008, Vol. 116, Paper 08-043(05), P641-652**
17. **Chisamera, M; Riposan, I; Stan, S; Skaland, T, "Effects of residual aluminum on solidification characterists of un-inoculated and Ca/Sr inoculated grey irons", Journal: Transactions of the American Foundry Society V 112 Paper No 04-096 P 867 - 877 (11p)**
18. **Sparkman, D A; Bhaskaran, C A, "Chill measurment by thermal analysis", Journal: Transactions of the American Foundrymen's Society V 104 Paper 96-127 P 969-976, 1996 (8 p)**
19. **Popescu, M.; Zavadil, R.; Sahoo, M., "SiC-The Most Efficient Addition to Increase the Nodule Count in Ductile Iron", Journal: International Journal of Metalcasting, Vol. 3, Issue 1, Winter 2009, P53-63**
20. **Barlow, J O; Stefanescu, D M, "Computer-aided cooling curve analysis revisited", Journal: Transactions of the American Foundrymen's Society V 104 Paper 97-04 P 349-354, 1997 (6 p)**
21. **Gloria, D; Gruzleski, J E, "Time as a control parameter in determination of grain size of 319 Al-Si-Cu foundry", Journal: Transactions of the American Foundrymen's Society V 107 Paper No 99-58 P 419-424, 1999 (6 p)**
22. **Lynch, P.C.; Voigt, R.C.; Furness, Jr., J.C.; Paulsen, D., "The Effects of Non-Contact Acoustic Stimulation on the Solidification Behavior and Microstructure of Aluminum Alloy A356", Journal: Transactions of the American Foundry Society, Vol. 118, Paper No. 10-088, P 57-68, 2010**
23. **Riposan, I; Chisamera, M; Kelley, R; Barstow, M, "Magnesium-Sulfur relationships in ductile and compacted graphite cast irons as influenced by late sulfur", Journal: Transactions of the Ameri-**

can Foundry Society V 111 Paper No 03-093 P 869-883, 2003 (15 p)
24. Popescu, M.; Zavadil, R.; Thomson, J.P.; Sahoo, M.; Gassere, P., "Studies to Improve Nucleation Potential of Ductile Iron When Using Carbidic Ductile Iron Returns", Journal: AFS Transactions 2007, Vol. 115, Paper 07-079(05)
25. Sadayappan, M; Thomson, J P; Elboujdaini, M; Gu, G P; Sahoo, M, "Grain refinement of permanent-mold cast copper-base alloys – final report", Journal: Canmet materials technology laboratory report MTL 2004-6(TR-R)
26. J. Tartera, M. Marsal and G. Varela-Castro, E. Ochoa de Zabalegui, "Looking at graphite spheroids", International Journal of Metalcasting/Fall 09
27. Personal conversations with Matthew Meyer and Michael Riabov, both working on this project.
28. D. Apelian, G.K. Sigworth, K.R. Whaler "Assessment of grain refinement and modification of Al-Si Foundry alloys by thermal analysis", Journal: AFS Transactions 1984, paper 84-151, page 297-307.
29. L. Bäckerud, G Chai, J. Tamminen, "Solidification characteristics of aluminum alloys, Volume 2, foundry alloys" AFS/Skanaluminium (1990)
30. S.A. Musmar, F. Mucciardi, J. Gruzleski, F. Samuel, "Investigation of Iron and Copper Intermetallics in 356 Aluminum Alloy and in Al- 7% Si Binary Alloy by an In-Situ Thermal Analysis Probe", AFS Transactions 2006

DERIVATIVE THERMAL ANALYSIS TERMS

Common Term	Computer/Mathematical Definition	Explanation
Temperature curve	Smoothed readings from the thermal couple in the sample cup.	This is the temperature of the metal plotted over time.
RoC – Rate of cooling curve	$1/1^{st}$ derivative	The scale and shape of this curve is easier for non-technical people to understand than the first derivative.
Zero crossing positive or negative	Behavior of a derivative curve easily programmed into a computer. If ((X_1 <=0.0) and (X_2 >=0.0) or((X_1 >=0.0) and (X_2 <=0.0) then ZeroCrossing:= True; // Pascal code	The definition of a zero crossing of a derivative curve crossing the zero line in either a positive or a negative direction locates a minimum or a maximum of the previous derivative.
Maximum or minimum of a derivative	Highest or lowest point of a derivative in a localized area defined by the zero crossing of the next higher derivative.	This defines the highest slope, either positive or negative of the next lower derivative in the area of the curve.
Maximum Temperature	Initial Positive Zero Crossing of the rate of cooling curve	This is an artifact: the highest temperature that the TA curve sees. It should be below the thermal couple melting point which is 1390˚C or the thermal couple may fail.
Start of Thermal Analysis	Initial positive zero crossing of the second derivative after the maximum temperature.	This is the first and highest maximum of the rate of cooling curve, and the beginning of non-artifact arrests. The TA system has stabilized and all arrests after this point are real.
Growth Temperature	Negative zero crossing of the RoC	Phases that undercool will then reheat (recalesce). This is the maximum temperature reached by the temperature curve, but may be lower than the true temperature, due to rapid heat loss. A true value will evidence itself by being flat on the top, as if the curve is hitting a ceiling, or a maximum temperature that it cannot exceed.
Strongest point of an exothermic crystalline phase arrest or phase change	Negative zero crossing of the 2^{nd} derivative or minimum of the 2^{nd} derivative as defined by negative zero crossing of 3^{rd} derivative	This is the temperature usually given for a crystalline phase precipitating out.
Strongest point of an endothermic void or shrink, or stress creating arrest	Positive zero crossing of the 2^{nd} derivative or maximum of the 2^{nd} derivative as defined by positive zero crossing of 3^{rd} derivative	This is the temperature usually given for this kind of arrest. The Solidus arrest is generally of this kind.
Start of an arrest	Positive zero crossing of 5^{th} derivative for quiet arrests, 4^{th} derivative in noisy conditions for exothermic phases, reversed for endothermic events	This is simply the beginning of the beginning of the inflection of the rate of cooling curve. This is the starting point for energy integration to measure the amount of heat being released (latent heat) or adsorbed by the arrest.
End of an arrest	Negative zero crossing of 5^{th} derivative for quiet arrests, 4^{th} derivative in noisy conditions for exothermic phases, reversed for endothermic events	This is the ending of the bending of the rate of cooling curve. It is the end of the energy integration to measure the amount of heat being released (latent heat) or adsorbed by the arrest.